Puncture Evaluation of the Scale Model

K.S. Seo, J.H. Ku, D.K. Min and S.G. Ro(1)
S.I. Hong(2)

(1)KAERI, Taejon, KOREA
(2) Chungnam university, Taejon, KOREA

SUMMARY

This paper describes a comparison between a puncture test and a FEM analysis in the case of a scale model dropped in the horizontal position. The deformation, strain and acceleration data due to the scale model tests were compared with the analysis results of the computer codes. The FEM analysis was used as a DYNA3D code, capable of simulating the mechanical behavior of the penetration effect. Its purpose was to verify the analysis methods. The total energy calculated by the empirical equation was reviewed with the results of the FEM analysis.

INTRODUCTION

The puncture test of the transportation casks was performed in accordance with the IAEA Safety Standards and domestic regulations. The specific condition of the puncture test is one of the hypothetical accident conditions. The regulations require that casks are able to survive punctures tested by the free drop of a cask from a one-meter height onto a 15cm diameter mild steel pin. The structural integrity of the scale model under the puncture condition was evaluated to perform the test and analysis.

The puncture test was performed using a one-third scale model. As the scale model was dropped in the horizontal position onto the mild steel pin, this pin made contact with the axial center of the outer shell and the neutron shielding materials. Instrumentation was made in the puncture test to get information regarding such areas as the strains and accelerations. During a puncture event, the plastic strain energy of the outer shell, intermediate shell and neutron shielding materials contribute to the impact absorbing. The outer shell and neutron shielding material are penetrated by the steel pin if the neutron shielding material is made of a silicone mixture that is weaker than the epoxy resin of a general neutron shielding material.

Nonlinear dynamic analysis was carried out using the DYNA-3D computer code. This computer code presents the explicit scheme in the time integration and shows the penetration shape through the application of the failure mode. The results of the computer analysis were compared with those of the empirical equations. These empirical equations, used in designing the cask shell thickness, were also generally used to meet the puncture resistance requirement. In the empirical equations, it is assumed that the backing material of the steel shell is lead. Therefore, these

equations are not appropriate for the application of a scale model having a silicone mixture as a backing material.

PUNCTURE TEST

A prototype cask is capable of transporting 7 PWR spent fuels and has a weight of 75 tons. The scale model was made of the same material as the prototype's, and all dimensions were scaled down linearly to one-third the size. The scale model was made of stainless steel 304, a lead and silicon mixture. The silicon mixture was sandwiched between the outer shell and intermediate shell, and the lead between the inner shell and intermediate shell. The thickness of the outer-, intermediate- and inner shell was 3 mm, 13 mm and 5 mm, respectively.

The drop test facilities consisted of a drop tower, a hoist , a release mechanism and a drop target with a 100 mm thick steel plate laid on the concrete foundation, as shown in Figure 1. A steel pin installed on the steel plate had a 50 mm diameter and 80 mm length. The one-third scale size of the steel pin is the same as the scale ratio of the scale model to prototype cask, as specified in IAEA Safety Series no. 37.

Four strain gages were applied to a single type and one strain gage to a Rossette type in the hoop and axial directions. Two accelerometers were applied to a piezoelectric type in the vertical direction. Strain and acceleration data were acquired through an amplifier, a data recorder and an A/D converter. The scale model was dropped from a 1 m height onto the steel pin. Due to the drop of the scale model in the horizontal position, the upper side of the steel pin contacted perpendicularily with the outer shell of the scale model.

The scale model was very severely deformed by the puncture events. The outer shell was cut off in the same size as the section of the steel pin and its dent depth was 14 mm. The deformed shape was a truncated cone type with a 120 mm radius from the center of the steel pin. The silicon mixture layer was penetrated perfectly and the intermediate shell was deformed. As total dent depth was 70 mm, the dent depth of intermediate shell was 21 mm if the undeformed thickness of the silicone mixture and the outer shell were considered.

Longitudinal and hoop strain gages were installed on the outer shell near the puncture face. Their maximum strain was about 954 $\mu\varepsilon$, as shown in Figure 3. Figure 3 shows that the hoop strain has discontinuity at 10.2 ms. At this location, the hoop strain varied steeply because the outer shell was fractured by the steel pin. It takes 5 ms from the initial impact instant to the fracture. A Rossette gage was installed on the intermediate shell perpendicular to the puncture face. The strain data of the Rossette gage had two peaks during the puncture event. First, a smaller peak took place in the impact of the outer shell and a second larger peak took place in the impact of the intermediate shell.

Accelerometers were installed on the intermediate and inner shell perpendicular to the puncture face, respectively. However, the g-value was represented coarsely because the predicted acceleration was decided to be very large. The impact of the intermediate shell was larger than that of the inner shell, as shown in Figure 5.

Maximum strain data were calculated in consideration of the initial offset voltages in Table 1. The maximum strain is represented on the right side of the puncture face, as the gage installation is the nearest to it.

FEM ANALYSIS

Computer analyses of the finite element method were performed in the beginning stage with only a large deformation as the plastic behavior. However, the outer shell and silicone mixture were penetrated by the steel pin in the puncture test. Therefore, nonlinear dynamic analysis was carried out in the final stage using a LS-DYNA3D computer code based on an explicit time integration scheme.

The analysis model of this finite element method was the same size as the test model and consisted of 11368 elements of a 3-dimensional solid type. A half size model was used, which was split by the plane, including the longitudinal axis of the cask and steel pin, as shown in Figure 6. The boundary condition was only free on the drop direction of this plane. A part of the outer shell and upper side of the steel pin were applied to the contact element type.

The dynamic data of material properties that the yield strength and the elastic modulus are increased due to the strain rate, were applied in order to compare with test results. The yield strength and elastic modulus of the stainless steel were 2.5858E8 and 1.97E11 Pa, respectively. The values of the silicone mixture were 6.11E6 and 1.28E7 Pa, respectively. As the puncture behavior of the outer shell became a failure mode by the steel pin, the application of the 19% failure strain in the stainless steel 304 was considered to get the penetration effect of the outer shell. The loading conditions were imposed by a velocity of v=4.429 m/s for the cask and v=0 for the steel pin.

In the FEM analysis, the longitudinal and hoop strain data near the puncture face had two peaks, one being the failure behavior of the outer shell and the other being the large deformed behavior of silicone mixture, as shown in Figures 7 and 8. The inner shell kept within the elastic limit during the puncture events. The total energy was about 14000 newtons-m because of a half size of a prototype. Maximum deformed depth was 32.4 mm in the puncture position.

SIMPLIFIED CALCULATION

It is important to determine the shell thickness in order to prevent the loss of the lead shield in the successive fire test. In general, the Nelms equation is applied as follows in the case of cylindrical shells with lead backing material, presented by L.B. Shappert. Assuming that E is directly linearly proportional to σ_u, the potential energy $E = W(h + \delta)$ can be expressed in its nondimensional form $\overline{E}$ as :

$$\overline{E} = E/\sigma_u t^3$$

W : the total weight of the cask
h : the drop height
δ : the maximum displacement after the punch initial contact
σ_u : the ultimate tensile strength of the outer shell

The use of this Nelms empirical puncture equation in cylindrical cask design may result in a nonconservative design. The unit of the following equations is lb-inches:

$$\overline{E} = 2.3x^{1.6}$$

$$x = \frac{d}{t}$$

d : the diameter of the puncture mild steel pin
t : the shell thickness

Another empirical puncture energy equation by R.C. Shieh predicts a stronger cask puncture resistance than that which Nelms equation has been developed. These test data for the dynamic puncture can be closely fitted into a set of curves represented by the equation in the case of the leaded shielded carbon steel model.

$$\overline{E} = 1.8(1+y+46y^2)e^{2/x}x^{1.3}$$

$(30y \le x \le 12;\ 0.067 \le y \le 0.2;\ z=1/24;\ \bar{l} = 2 \sim 3)$

$$y = \frac{d}{D},\quad z = \frac{r}{d},\quad \bar{l} = \frac{l}{D}$$

D : the outer diameter of the cask shell
r : the edge radius of the steel pin
l : the cask length

By application to the intermediate shell of the scale model, the calculated results for the potential energy, Nelms and empirical equations are 31609, 23165 and 34123 newtons-m , respectively.

DISCUSSION OF RESULTS

In the first stage of the puncture test, the outer shell was penetrated after it was deformed to a shape of truncated cone type. In the second stage, the behavior of the silicone mixture was similiar to that of the outer shell and finally, the intermediate shell was dented by the steel pin. As the diameter of the dent area was 2.4 times that of the steel pin, this area needed a detail mesh generation for FEM analysis. A general neutron shielding material was used as epoxy resin type that this compression yield strength is 6.05E7 Pa. The silicone mixture did not have an energy-absorbing characteristic during the puncture event because its yield strength had only 2% that of the stainless steel and 10% that of the general neutron shieding material.

In FEM analysis, a general computer code was restricted to the simulation of the 3-dimensional penetration effect. If the penetratraion effect is not considered, the steel pin does not arrive at the intermediate shell, and the outer shell and the silicone mixture are only deformed. The analysis results indicate that the puncture behavior is correctly predicted by the DYNA3D computer code. The total energy is a little smaller than the potential energy because the cooling fins are ignored and the total weight was reduced.

In simplified calculations, the Nelms and empirical equation are under- and over-estimated in comparison with the potential energy. Similarily, the thickness calculations are not appropriate. The calculated total energy of the FEM, Nelms' and empirical equation are 12% smaller, 26.7% smaller and 8.0% larger than the potential energy, respectively.

CONCLUSION

Initially, we decided that the containment is bounded on the inner shell and lid. Therefore, the integrity of the inner shell keeps on within the elastic range though the outer shell and silicone mixture are partially lost and intermediate shell are deformed.

In the case of the FEM analysis applied to the silicone mixture used as the neutron shielding material, the penetration effect of the outer shell and silicone mixture must be considered because the plastic dissipation energy of the two materials, including the failure, is smaller than the total potential energy of the puncture event and consequently, the intermediate shell was deformed.

REFERENCES

L.B. Shappert, A Guide to the Design of Shipping Casks for the Transportation of Radioactive Materials. USAEC Report ORNL-TM-681. (April 1965)

R.A. Larder and D.F.Arthur. Puncture of Shielded Radioactive Material Shipping Containers Part I - Analysis and Results. NUREG/CR–0930 PT I. (December 1978)

R.A. Larder and D.F.Arthur. Puncture of Shielded Radioactive Material Shipping Containers Part II - Static and Dynamic Tests of Laminated Plates NUREG/CR–0930 PT II. (December 1978)

R. C. Shieh. Empirical Equations for Puncture Analysis of Lead-Shielded Spent Fuel Shipping Casks. the 5th PATRAM vol. 2 (May 1978)

Ting-Yu Lo. Puncture Evaluation of Shippingport Package. UCRL-99652 (May 1989)

D. Moulin, L. Tanguy, B. Aufaure. Puncture Test of a Package - Comparison between Experimental Test and Dynamic Analysis. CEA-CONF--10344 (Jun 1990)

J. Altes, H. Geiser, W. Volzer, A. Frenk and G. Deeken. Finite Element Analysis for the Impact Behaviour of a Cask Interacting with a Rigid Pin. SMiRT-12 (1993)

Jim Liu and Shen Yi Luo. A Numerical Study of Transportation Casks Subjected to Puncture Loads. International Conference on Nuclear Engineering vol. 5 ASME (1996)

T.R.Bump and Y.Y.Liu. A Simplified Analysis of the Regulatory Puncture Test. CONF-951203 --67. (1996)

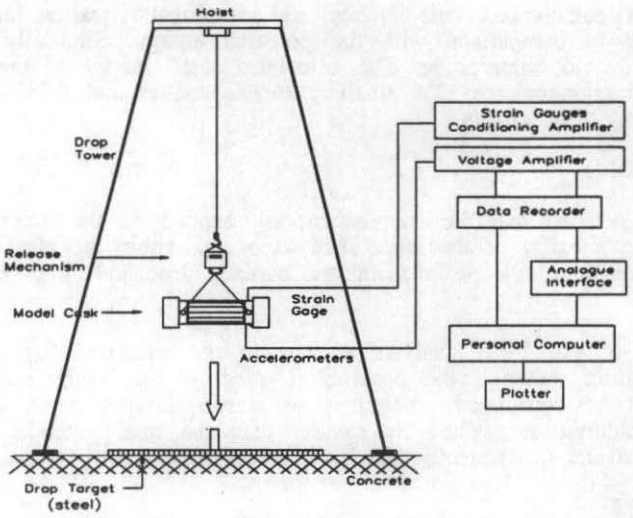

Figure 1. Test Facility and Data Acquisition System

Table 1. Maximum Strain Data

Location (from the puncture)	Direction	Maximum Strain(με)	Time(ms)
Right side	Longitudinal	186	9.9
Upper side	Longitudinal	367	14.9
Upper side	Hoop	498	22.2
Right side	Hoop	954	10.2
90 ° rotation	45 ° right	486	30.3
90 ° rotation	Longitudinal	453	28.6
90 ° rotation	45 ° left	229	23.6

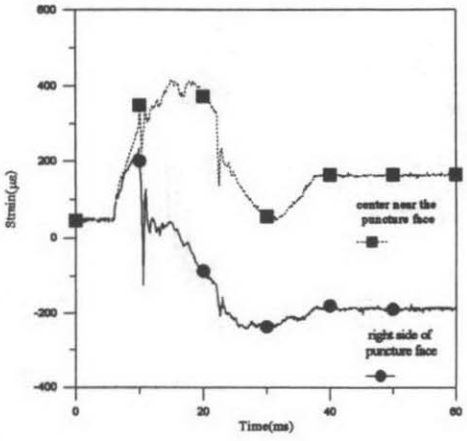

Figure 2. Longitudinal Strain Data of Single Gage

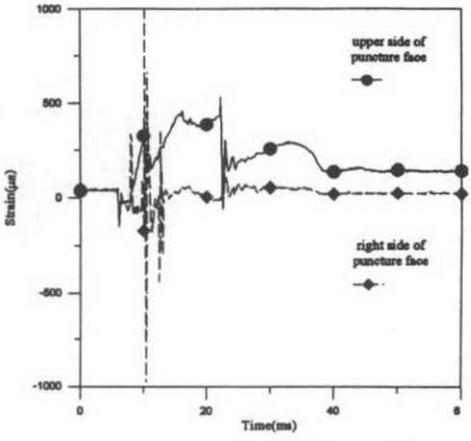

Figure 3. Hoop Strain Data of Single Gage

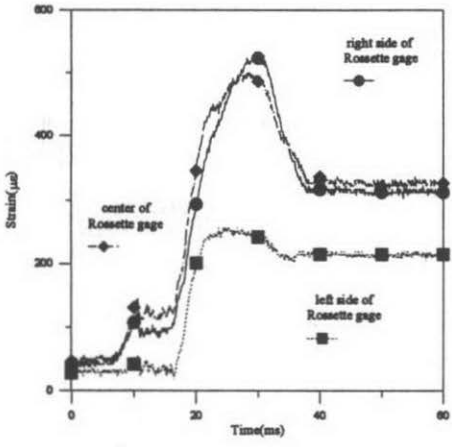

Figure 4. Strain Data of Rossette Gage

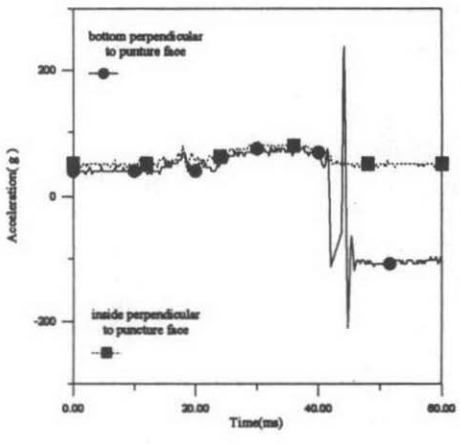

Figure 5. Vertical Acceleration Data

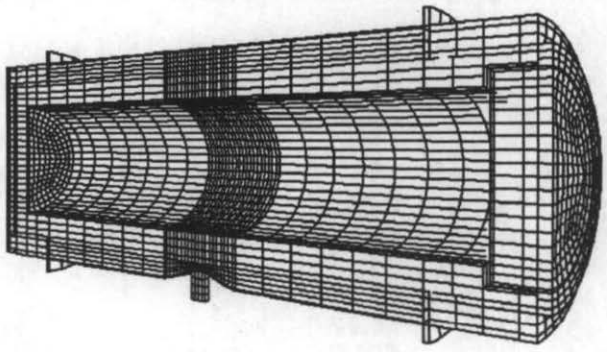

Figure 6. Deformed Shape Simulated by DYNA3D Computer Code

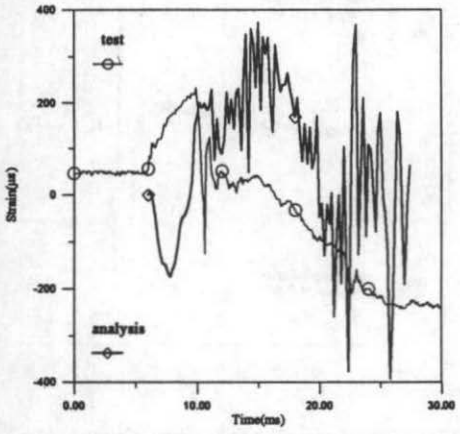

Figure 7. Comparison with Analysis and Test in Longitudinal Strain

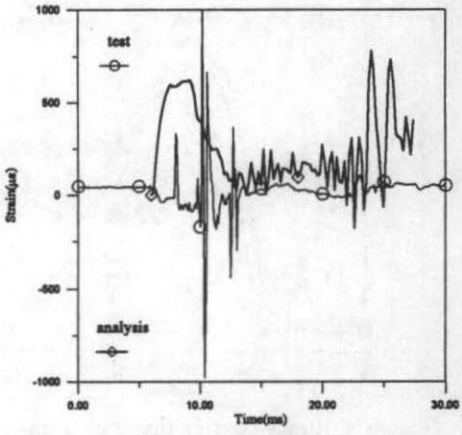

Figure 8. Comparison with Analysis and Test in Hoop Strain